Extracting cell and fibre orientation from microscopic images: computational methods and tools

Medha Sharma[1,2]

[1]Department of Instrumentation and Control Engineering, V.E.S. Institute of Technology, University of Mumbai, Mumbai 400 074, India
[2]Indian Institute of Technology Bombay, Powai, Mumbai 400 076, India

Orientation of cell and its actin fibres dictate various properties of the cell and its associated tissue including morphology, cell migration and response of cell to external stimuli. While the vital role of cell and actin fibre orientation has been demonstrated in various studies and across many cell-types, extracting this information from microscopy images is a challenging task. Although several methods have been developed to quantify alignment of a cell and its actin fibres from experimental images, all of them differ at one step or the other. We highlight the importance of orientation of cell and associated fibres and present a generic scheme of various approaches to assimilate the widely used methods. We have presented a systematic approach to determine cell and fibre orientation. The study will improve our understanding of the core processes and will also help in development of high throughput imaging methods to extract information from experimental images.

Keywords: BEAS, cell orientation, DFT, fibre orientation, FFT, image processing, thresholding.

IN the study of biological phenomena, cell is at a very fundamental level, as it is the smallest building block of all organisms. In fact, it is the smallest form of life that exhibits all the basic traits that form life such as birth, ingestion, digestion, protection and finally death. Cell during its life cycle experiences a number of mechanical interactions with surrounding environment necessary for its communication, proliferation, differentiation and migration[1–8]. A cell responds to these mechanical forces by exhibiting changes at various levels such as in morphology, protein synthesis[9,10], gene expression[11,12], etc. Then, cell tries to adapt to its environment through these changes. Several of its mechanical properties facilitate the adaptation of cell to the associated environment. Therefore, to understand the mechanism of working of a cell, knowledge of its mechanical properties and how do these get affected by a cell's surrounding environment is very vital. Microscopy-based imaging and its subsequent analysis is one of the traditional and widely used approaches to gain insights into the cell's mechanical and morphological properties. While microscopy imaging is a widely used approach to extract quantitative information about cell morphology, image analysis and morphology quantification are still challenging. One of the morphological features of a cell, which has been shown to exhibit several genotypic and phenotypic properties of a cell is the orientation of the cell. Similarly, orientation of fibres has been shown to exhibit various properties of associated cell population, including their density, topography, etc.

The orientation of cell and the associated fibres are the indicative of many physiological and disease conditions. While microscopy-based image acquisition is the traditional method to gain insights into the orientation and morphology of cell and associated fibres, extracting thequantitative information about the cell or fibre orientation from these images is a challenging task. Although with the advancement in image processing, new methods to extract information have been developed, most of these methods have limitations in their scope of application. Also, in addition to different approaches for analysing images, different metrics have been proposed to represent the orientation of cell and fibre in a quantitative manner. Different approaches to extract information about the orientation of cell and fibres have been discussed. Limitations and shortcomings of these approaches are also discussed here. Further, in addition to core algorithm to quantify the orientation, the importance of pre-processing and post-processing is also highlighted.

Various methods for quantification of cell orientation and extracellular matrix (ECM) fibre orientation have been discussed here. The organization of the paper is as follows: the first section highlights the importance of orientation of cell and fibre in current biological studies. It discusses the importance of cell-alignment and fibre alignment in *in vivo* systems. The following section elaborates the unified approach to quantify the cell orientation. Particular methods along with their merits/demerits are also discussed. The later section is focused on understanding and evaluating different fibre alignment quantification methods. Finally, the article concludes with highlighting some of the open problems in the field.

e-mail: medhasharma7575@gmail.com

Importance of cell alignment and fibre alignment in biology

Organization of cells within a tissue dictates the anisotropy of its ECM in the spatial setup and together they characterize the tissue and the organs that they make up[13]. Alignment of tissue cells plays a key role in various important functions of the tissues such as neuron regeneration, defining mechanical and physical properties of tissue, pattern formation in embryogenesis, tissue maturation, etc.[14–22]. Further, given the increasing use of regenerative medicines and tissue implant, the understanding of tissue functioning has become very important. Only once understanding of the tissue functioning is clear, engineered muscle tissue with effective functioning and capabilities to bear the physiological load and stress can be developed. To realize most of the complex tissue functioning, the engineered tissue must be designed in such a way that the cells of engineered tissue mimic the alignment of the native cells of that particular tissue[23]. Next, stress fibres represent the internal structure of the cells. Angular distribution and direction of these stress fibres influence cell properties such as shape, size, etc. as well as its response to various external cues, e.g. increase in stress or strain[24,25]. Thus, stress fibres regulate a large set of cell properties and therefore the overall behaviour of the tissue. To further highlight the importance of cell and stress fibre orientation, the following are some of the specific examples of *in vivo* systems.

Muscle tissue

All muscle cells are required to possess the ability to undergo contraction and stretching. Contraction and stretching require generation of forces, which in turn, requires proper cell alignment. For e.g. rod-shaped muscle cells have highly organized myofilaments which are critical for proper functioning of muscle tissue. Pharmacologically, the disorder in the musculoskeletal system causes disturbances in the alignment of muscle. This can be used to understand the nature of a musculoskeletal disorder. One of the most complex structures of human body, the heart, has its muscle cells aligned in a complex spatial distribution to enable strong ductility for beating of the heart[26]. Since current conducts fastest in the long axis of cardiac fibres[27], the electrical conductivity of heart depends greatly on its fibre orientation. Conversely, pathological hearts have disoriented thick, short and fragmented fibres[23].

Vascular tissue

Blood vessels have high tensile strength and flexibility to facilitate the pulsatile flow of blood. During vascular remodelling and angiogenesis, the strain exerted by this flow of blood leads to cellular alignment. This, in turn, alternates between two smooth muscle cell (SMC) phenotypes: contractile and synthetic. While a contractile phenotype is required for proper functioning, in vascular disorders such as hypertension, SMC may switch the phenotype to a synthetic one. In addition, endothelial cells have been shown to be oriented in the direction of longitudinal axis of the vessel. These cells align intracellular cytoskeletal components according to the stress due to blood flow. The stress due to blood flow has been shown to play a pivotal role and cells which are not able to adapt to it properly may cause many disorders in several central processes including vascular remodelling, physiological control of vessel diameter, alternation of vascular permeability, and the pathological consequence of cardiovascular disorders[28].

Nerve tissue

Schwann cells (SCs) protect, hold, insulate and provide immunity to neurons from pathogens and dead neurons. For guided axonal re-growth, alignment of SCs and ECM is essential. Hence, it is important to determine the orientation of SCs and ECM to determine the physiological and pathological conditions of the tissue.

Collectively, all these examples (and such other examples) highlight the importance of cell and stress fibre alignment in the biological systems. So, to understand the physiological or disease state of a cell/tissue systems, it is important to know the alignment of its cells and associated stress fibres.

Determination of cell orientation

Owing to the importance of cell orientation in maintaining proper functioning of biological systems, a number of ways have been devised to quantify the orientation and alignment of cells. Methods to quantify both the alignment of an individual cell and the orientation distribution in a group of cells/tissue have been developed. Determination of orientation of cells involves many stages. Different methods have been devised to address a specific problem. We have tried to assimilate the various methods and provide a generic step-wise method to quantify the cell orientation.

Figure 1 provides a step-wise generic procedure of determination of orientation distribution of cells. The initial stage involves acquiring the image of the cell using various microscopy techniques such as phase contrasts, fluorescent microscopy, etc. Thereafter, pre-processing of images is done for making them ready to be used for segmentation of cell, i.e. detection of the cell image. Next step involves calculation of its alignment and finally its relative alignment with other cells giving overall orientation distribution.

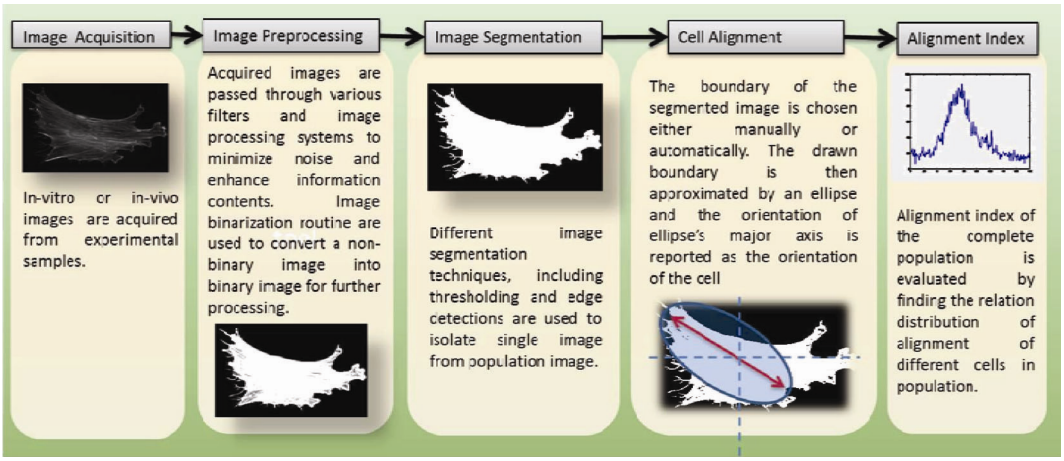

Figure 1. Determination of cell orientation. The image is acquired and pre-processed for de-noising and improving its quality. The cell is segmented out and its boundary is approximated as ellipse. The angle which ellipse's major axis makes from x-axis provides orientation of cell. Thereafter, alignment index of the whole population can be quantified.

Image acquisition and preprocessing

Microscopy images are generated from various experiments. The nature and type of experiments highly depend on the nature of the study. Live cell imaging where the image is taken after a constant time-slot is often used to study the cell migration/invasion dynamics. Lee *et al.*[29] have used live cell imaging to study the cell migration properties of transformed metastasis breast cancer cells MDA-MB-231. In contrast to live cell imaging, one-time-point experiment where the image is taken after a particular time (e.g. after 1 day or 2 days, etc.) is performed to study the long range effects of drug or environment factors (e.g. role of substrate stiffness). Tilghman *et al.*[30] studied the effect of increase in cell substrate (from 150 Pa to 4.8 kPa) on cell surface area (for A459, MDA-MB-231, PC-3 and mPanc96 cell lines) by imaging the cells after 20 h (ref. 30). Irrespective of the type of experiment, before analysing the orientation of cells from the obtained image(s), the quality of captured image needs to be improved by various image-preprocessing methods such as applying filters so as to suppress the noise, equalizing the intensity throughout the image and enhancing the contrast.

Segmentation of cell

Segmenting the cell from an image is the first major step to finding its orientation. While the efficacy of segmentation method highly depends on the properties of the cell under consideration, here we analyse the various prominent methods being used for the purpose. The key property being exploited for segmentation of the cell is the difference in the contrast of the cell from the background image. A number of methods have been used to quantify the gradient of intensity in the image and find an appropriate threshold to separate the cell from the background. This threshold is the major accuracy contributor in the process. Hence, much work is done to achieve a refined threshold value. Once this is achieved, a binary mask is applied to the image to segment out the cell. Thereafter, post-processing is done to fill holes inside the mask and obtain the outline of the cell which can then be smoothened and isolated from other objects in the image (e.g. noise effects and incomplete cells).

Global versus local thresholding

Thresholding partitions the image in such a way that one part has pixels above the defined threshold and the other has below it. Thresholding can be 'global' or 'local'. Global thresholding defines a single threshold for the entire image. The major complexity involved with segmentation of cells from the image is that the intensities of the cell and background overlap with each other and variation is not constant throughout the whole image, that is, at different areas in the image, the cell and background intensities vary. Hence, global thresholding cannot be effective for segmentation purpose, making it essential to extract local areas to reduce the complexity of thresholding. To do so, variance in intensity of cell in the image and variance in intensity of background pixels can be measured as cell-pixel variance V_c and background-pixel variance V_b respectively, to quantify the complexity which arises from intensity variation[31].

The high value of either V_c or V_b or both shows the overlapping in the cell and background intensities, thereby increasing the difficulty or complexity in the segmentation process. It has been found that extraction of an area from the original image for thresholding decreases the value of both V_c and V_b, representing ease in segmentation. Also, the contrast in the image, i.e. ratio of average cell and background intensities is of importance while performing segmentation process, but by extracting a

patch, contrast does not get affected significantly. So, windows or patches from the original image are extracted out according to the distribution of the cells in the image to ease processing. Then, according to the features of the image, threshold for different patches needs to be estimated for further processing.

Thresholding

Many methods and algorithms have been devised for thresholding. Many imaging techniques have also been developed to mitigate the problems in the process, specific to the requirement. Learning-based algorithms have also been tried in this field but they require much training and manual work. Manual methods, though reliable, suffer from low efficiency when there are hundreds of cells involved. Moreover, they are very time consuming and tedious. They also suffer from inter-operator variability. Many other approaches have been tested, mainly, Huang[32] (measures fuzziness and Shanon entropy), Li[33] (minimizing cross-entropy), max entropy (ME)[34] (uses entropy of histogram), Otsu[35] (minimizes weighted sum of variance of two classes), Shanbhag (SH)[36] (entropy-based approach), Yen[37] (discrepancy between thresholded image and original image as well as the size of the same are considered here) and binarization-based extraction of alignment score (BEAS)[13] (uses mean and standard deviation for local thresholding). For defining the threshold, these approaches have exploited different features of the image as mentioned. Out of all these various approaches, it has been found that the approaches giving results close to the true value are Huang, Li and BEAS, with the BEAS being the most effective than other two[31]. Furthermore, BEAS method is reportedly having more advantages and reliability than many automated methods such as Fast Fourier Transform-Radial Sum[38] (FFTRS) and gradient-based approaches[39]. The later ones are not able to give good results even for perfectly aligned cells. Alternatively, the thresholding accuracy varies as FFTRS < Gradient < BEAS. In BEAS method, algorithmically, the image is first pre-processed by passing through a despeckle filter to reduce the effect of signal-pixel noise, then it is passed through Gaussian band-pass filter as it removes high-frequency components and also removes noise due to components other than the cell as well as the effect of uneven illuminations. These features are implemented using ImageJ program developed by US National Institutes of Health (NIH). The threshold is calculated using

$$T = m + km\left(\frac{s}{\sigma} - 1\right), \tag{1}$$

where T is the threshold, m the mean intensity, k the tuning parameters, s the standard deviation, and σ, the maximum standard deviation.

Here, the mean value, m can be considered as the reference value and $km((s/\sigma) - 1)$ as the shifted value. Hence, the shifted part will define the accuracy of the threshold value and it is dependent on the mean and standard deviation only. However, for certain images, the cell distribution may have same mean and standard deviation, but have different optimal threshold values[31].

Afridi *et al.*[31] proposed an improvement to this method by exploiting the rate of increase of pixel intensity from low values to peak values as another characterizing factor, because for same mean and standard deviation, this rate α can be different[31]. The threshold in this method is calculated for different patches of images through pixel intensities x and corresponding pixel count y, considering only the distribution towards the left of the most frequent intensity (m_f). Most frequent intensity is calculated from the mode-intensity of each of the considered patches. Additionally, the following equation is used to measure the rate of rise by employing exponential distribution

$$y = Ae^{\alpha * x}, \tag{2}$$

Now to refine the threshold value, instead of using the mean value m, the most frequent intensity value m_f could be used as this is the value beyond which the intensity never rises. Also, the shift part can be improved by utilizing the α and using suitable values for tuning parameter (k) (refer citation 31 for further details). Once an optimal threshold value is found, a binary mask is created to separate out the cell from the background by considering the pixels with brightness less than the threshold, as cells. Subsequently, the holes are filled and we obtain the boundary of the cell.

Post-processing of cell image

The intensity thresholding methods explained above are used as a first step towards further processing because the boundaries may not be very sharp and well-defined. Boundary may be slowly diffusing so that if the threshold is changed slightly, the output may significantly change. Therefore, other different methods are growing rapidly along with segmentation for achieving improved image for analysis. These methods include morphological filtering, region accumulation and deformable model fitting[40]. Morphological filtering utilizes mathematical morphology and is distinguished as binary and grayscale[41]. Binary morphology can be used for polishing coarse segmentation while grayscale is employed for enhancing image features as a pre-processing step. Region accumulation involves iteratively adding connected pixels. Many varieties of these processes have also developed, e.g. accumulating region from a pre-defined small region called as *seed*. Many improved versions of these have been developed such as, e.g. seeded watershed segmentation and

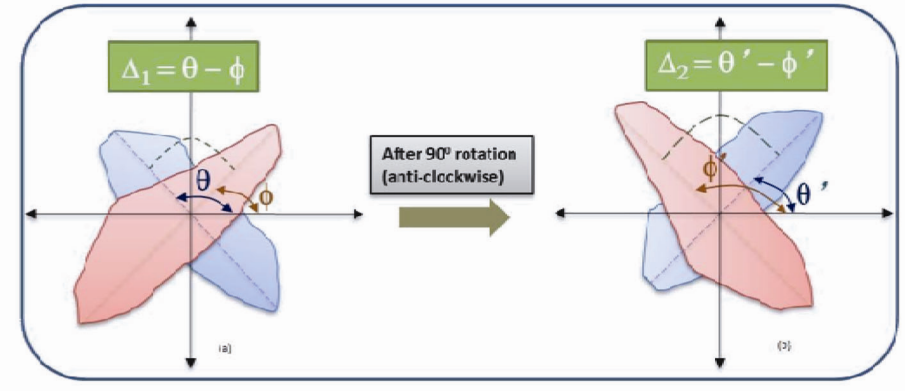

Figure 2. Orientation calculation: ***a***, Two cells with orientation angle θ and ϕ from x-axis in x–y coordinate system. ***b***, Same pair of cells when x–y coordinate system is rotated 90 degree in space.

edge detection segmentation[42]. Over-segmentation often occurs in these methods because of the high sensitivity of these algorithms. For instance, the watershed algorithm is very sensitive to gradient image sensitivity variations and hence noise in such cases can lead to a very large number of catchment basin resulting in over-segmentation[43]. For reducing this effect, region-merging technique could be used along with region accumulation[44]. There are several other known issues with seeded region accumulation techniques such as error due to noise and seed selection. These problems are addressed by using unseeded region growing and employing adaptive anisotropic filtering techniques for pre-processing of the image[45].

Orientation of individual cell

After segmenting out the cells from the image, the alignment of these cells is determined. The first step here is to find the pixels at the boundary of the cell by checking the pixel value corresponding to the boundary value. These are then fitted to the equation of an ellipse. The major axis of the ellipse will give the length of the cell while the angle ϕ from the x-axis will give the orientation of this cell. The area A of the cell is equal to the number of pixels in the cell. The centroid of the cell can be found by averaging the x and y coordinates of the pixels in the cell area. In this way, we can have area A and angle 'ϕ' of all the cells in the image (tissue).

Overall orientation of cell population

Once the values of area A and angle ϕ are known for all cells, depending upon the requirements, two quantities can be determined: (i) Orientation distribution: provides a measure of cells oriented in each direction; this gives relative alignment of cells with each other. (ii) Alignment score: provides a measure of cells aligned in some externally given direction.

In both cases, the relative angular position from a particular angle θ will be required. Figure 2 shows the orientation of two cells (viz. θ and ϕ) from the x-axis and the relative angle Δ given by $\Delta = \theta - \phi$.

Now in case 1 (Figure 2 *a*), assume $\phi = 10°$ and $\theta = 170°$, then, $\Delta = \Delta 1 = 160°$. In case 2 (Figure 2 *b*), the coordinate axis is just shifted by 90° and thereby $\phi' = \phi + 90° = 100°$ and thus, $\Delta = \Delta_2 = 20°$.

Practically, both the cases are same and so just calculating Δ is not sufficient; instead, a quantity is needed that treats both the above cases in the same manner. This issue is resolved by the following formula[13]

$$O(\theta) = \frac{\sum_n A_n \cos(2(\theta - \phi))}{\sum A_n}. \quad (3)$$

$O(\theta)$ will quantify the extent to which cells are oriented in direction θ. Now in this equation the term $\cos 2(\theta - \phi)$ resolves the above problem of relative angle, since in case 1 (left) the value of $\cos 2(\theta - \phi) = \cos(2\Delta)$, while in case 2 (right), the value of $\cos 2(\theta - \phi)$ becomes

$$\cos 2(\theta - 90 - \phi - 90) = \cos 2(\theta - \phi - 180)$$

$$= \cos(2\Delta - 360) = \cos(2\Delta). \quad (4)$$

Hence, the value remains the same in both cases, thereby, nullifying the effect of the rotation of coordinate axes. Also, since $O(\theta)$ is an even continuous periodic function, this helps prevent artifacts as well. Another beauty of this formula is that it takes weighted average of all the cells, this is helpful since not all the artifacts can be removed from the cell image and there may be some small region that is not actually a cell but is taken as one. Now in this formula, its contribution will be averaged out and will have very small overall effect (due to low area). On the other hand, if two cells are clubbed together and taken as

a single cell, then its contribution will be double in the overall orientation. Hence, this method directly corresponds to the cell density instead of individual cells. Now, the overall direction of the alignment is given by θ^* for which $O(\theta^*)$ is maximum. It will show that maximum numbers of cells are aligned in this direction. The value of $O(\theta^*)$ can vary from 0 to 1, with 1 showing perfect alignment, while 0 represents random orientation.

Determination of fibre orientation

The response of a cell to change in its environment heavily depends on the internal structure of the cell. One of the major components of the cellular structure is the network of actin fibres. A network of actin fibres controls various cell properties including its ability to contract, migrate and show mechano-sensitive responses. Therefore, understanding of structural properties of actin network is very important to understand the behaviour of a cell and to predict its response to external stimuli (e.g. drug-induced stimuli).

To establish a well-defined relationship between the response of the cell and its constituents to the environment, accurate measurement of the orientation of its actin fibres is also required. For obtaining orientation of actin fibres, many methods have been devised starting from measuring angles one by one. Given the fact that, unlike a cell, fibres are mainly one-dimensional (1D) and can be represented by a single frequency component discrete Fourier transform (DFT)-based methods have also been used to understand the orientation of these fibres. Actually, in the spatial domain, we have the luminance value and we can see images that our brain is familiar with; but in the frequency domain, the analysis is easier as we can obtain deeper information about the image. Moreover, the Fourier and time domain have almost inverse relationship, so what may not be clearly analysable in the time domain, may easily be analysed in the Fourier domain. For example, the higher frequencies show the sharp corners, the lower ones show the smooth details. Sometimes for analysis purpose, we may require cutting off sharp changes in an image or vice versa, such processes are easily done in Fourier domain by removing high frequencies or low frequencies correspondingly.

Fluorescent images and second harmonic generation (SHG) images obtained from confocal microscopy images are used to extract information about the fibre network structures such as cell actin stress fibres. Fast Fourier Transform (FFT)-based DFT is performed on these images. FFT is used as it requires much less computational time by reducing the number of operations substantially ($2n^2$ operations to $2*n*\log(n)$ operations). Figure 3 shows the details of the process of obtaining the orientation using DFT processes. Detailed explanation is provided in the following sections.

Image acquisition and preprocessing

For better implementation of DFT and to obtain accurate results, the main dependency is on the quality of images. Hence, much effort is used to improve the pre-processing part. Some of the approaches used include the application of gradient pyramid to reduce noise and CPU time and using despeckle and band pass filters. Apart from these basic approaches, SHG imaging along with analytical methods can be used to automate the process[46]. The use of this kind of imaging is encouraged by the fact that in the case of random orientation SHG will not be deducted because phase matching of electrical field required for SHG will not be present if molecules are disoriented. In general, electrical field produces polarization depending on permeability and susceptibility of the material and SHG uses this property and requires coherent scattering of the electrical field from all the molecules. However in the case of destructive interference, due to random orientation, no SHG is deducted. In particular, the strongest SHG signal is obtained when propagation plane of excitation beam of light is perpendicular to the fibres. SHG directionality and intensity is greatly influenced by fibre orientation. Once SHG images or the commonly used fluorescent images are obtained through microscopy, they are converted to 8-bit images. The image processing could be performed by using specific tools such as ImageJ or MATLAB according to the requirement. ImageJ is a very useful to extract biophysical information such as the surface area of cells, the circularity of the cell from the acquired images by manually masking (selecting) cells in the images. Due to the requirement of manual tracking, ImageJ is not an efficient tool for analysing a large number of cells. In contrast, MATLAB can be used to process a large number of cells by writing automation script which automatically load the image, process it and unload the image. This process can then be repeated for a bulk number of images without manual involvement. While this is a highly useful approach, it requires intelligent/complex algorithms for automatic image thresholding and masking thereby increasing the complexity of the 'processing' module.

Thresholding for fibre orientation

Many thresholding algorithms have been designed to reduce the signal-to-noise ratio similar to those previously used in cell orientation. However, since the object is different in this case, the algorithm needs to satisfy the requirement for fibres that can be considered as a 1D object. One such algorithm calculates the intensity of pixel (x, y) as: $I_{xy} = I_{xy} - I_k$, where I_k is the mean of all intensities in the square area surrounding the pixel[46]. The size of the square is determined by kernel k. If I_{xy} results in a negative value, it is taken as zero. This may result in

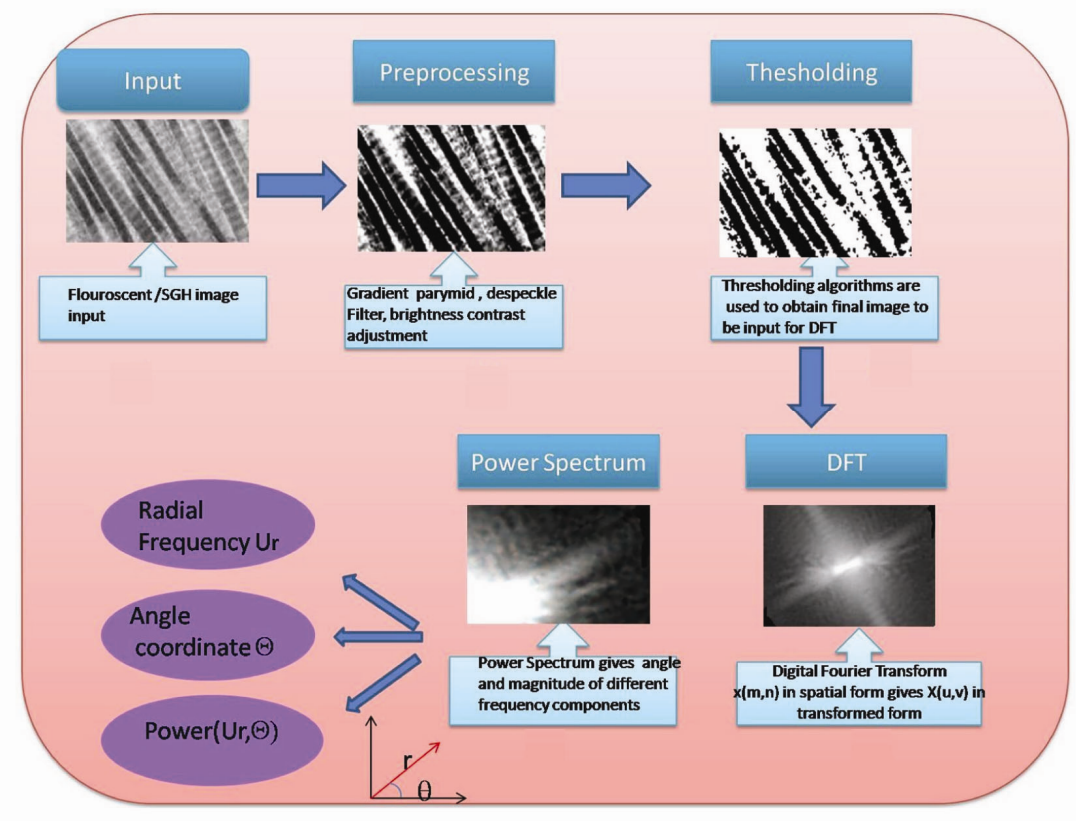

Figure 3. Orientation distribution of fibres. Input image is improved in terms of brightness and contrast. DFT is performed on the pre-processed image. DFT output is converted to give power spectrum which provides radial frequency, orientation and power magnitude. The resultant is improved by passing through band pass filter which provides only relevant frequencies.

better contrast depending on the intensity of fibre. If the intensity of fibre is very low, the effect of Gaussian noise may increase, i.e. the signal-to-noise ratio will decrease. To eliminate this, all the pixels which are not interconnected beyond a pre-defined number of pixels (taken as fibres), are set to zero. This will make sure that only well-defined fibres will be enhanced. In case the sum of mean and standard deviation are below the desired value, standard procedures of erosion and dilation from MATLAB functions (or equivalent function in other packages) could be implemented. Additionally, non-conventional approaches such as clustering-based methods[47] have been employed. In this method, an image is divided on the basis of correlation, i.e. clusters will be formed. Here, the seed of the clusters will be decided according to the intensity of light; for example, if 3 clusters are taken, then the one with highest intensity seed will be included as fibres, the one with the lowest intensity will be treated as the background and the remaining area will have its seed at the average intensity. Different algorithms exist for achieving the final segmented image of the fibres such as K-means clustering, fuzzy clustering, imperialist competitive algorithm. All these show competitive results in terms of quality of the image.

Applying DFT for fibre orientation

Next step in fibre orientation quantification is to apply DFT on the image matrix. Apart from simplified analysis in Fourier domain, DFT has the property that it is separable in the sense that two-dimensional (2D) DFT can be performed by doing 1D DFT twice; either by doing 1D analysis in x-direction, and then in y-direction or vice versa. 1D DFT is given as

$$F(u) = \sum_{m=0}^{M-1} F(m) e^{-j2\pi((u*m)/M)}. \tag{5}$$

To convert this to 2D DFT, this can be done twice using the *separability theorem* as follows

$$F(u,v) = \sum_{n=0}^{N-1} \left[\sum_{m=0}^{M-1} F(m,n)\, e^{-j2\pi((u*m)/M)} \right] * e^{-j2\pi((v*n)/N)}. \tag{6}$$

This equation can be used conveniently in 2D representation, which also centers the low frequencies.

$$F(u,v) = \sum_{n=1}^{N}\sum_{m=1}^{M} F(m,n)\; e^{[-j2\pi((u-1)(m-1)/M)+((v-1)(n-1))/N]}. \tag{7}$$

To implement this DFT on an image, the image is broken into spatial frequency components as the image has only space periodicity. Since the image is 2D, these components will be distributed in 2D space. DFT has the advantage of breaking up 2D DFT into 1D DFT for analysis. To understand how this helps to analyse fibre orientation, let us go to basics of DFT. In 1D signal, DFT simply gives frequency components with some low frequencies owing to the smoothness of the signal and some high frequencies resulting in peaks and changes. However, images are 2D, i.e. they have both horizontal and vertical components. On performing 2D DFT, we get frequencies from both horizontal and vertical counterparts. An image with no horizontal change will give only vertical frequency components since no frequency component will be present in the horizontal direction; similarly, an image with no vertical change will give only horizontal frequency component. Now from the above analysis, we can easily conclude that if the orientation of fibres is in a particular direction ϕ, then the frequencies will be distributed in direction 90° shifted from Φ. Hence

$$\phi = \theta + 90°. \tag{8}$$

In case of an image with both horizontal and vertical components, 2D DFT will have a resultant value of frequencies owing to both horizontal and vertical components. In the output image, we will observe values only on the pixels where frequency components are present and the value of the pixel will provide the magnitude of the frequency component. Further, since Fourier component is a complex quantity, each component will have a magnitude and an angle. To analyse both, we can map this to polar coordinates. The radial frequency and the angle from x-axis are given as

$$U_r = \sqrt{(u^2 + v^2)}. \tag{9}$$

$$\theta = \tan^{-1}\left(\frac{v}{u}\right). \tag{10}$$

This representation shows space frequency component as the distance from the origin and its angle from the horizontal represents the angle of that component θ (ref. 15). Orientation distribution of the components is determined via mapping the values of spatial frequencies with θ value, thereby giving $F(\theta)$. If the fibres are randomly oriented, this distribution curve will also be random with no specific peak. On the other hand, if fibres are well-oriented at a particular angle ψ, then a peak will be observed in the distribution curve. We can also determine the percentage of fibres oriented in a particular direction θ_m by the following formula[46]

$$O\%(\theta_m) = \left(2 * \left\{ \frac{\int_{-90}^{90} F(\theta)[\cos^2(\theta - \theta_m)\mathrm{d}\theta)}{\int_{-90}^{90} F(\theta)\mathrm{d}\theta} \right\} - 1 \right) * 100. \tag{11}$$

Post-processing for fibre orientation

To improve the output, band pass filter can be applied. As a result of this filtering, low pass effect will allow higher frequencies to be removed, thereby, removing the sharpness and finer details of fibre while preserving shape and orientation. On the other hand, high pass effect will remove orientation due to higher aspects such as clusters and hence focus will be on relevant frequencies. It has been found that the DFT frequencies that provide fibre orientation with the best accuracy are the ones within ± 10% of the frequency corresponding to the wavelength of twice the fibre width. However, processing error may be introduced due to many reasons such as truncated fibres, resolution of image, etc. The result can be improved by error minimizing techniques such as Von Mises distribution and by optimization techniques such as Monte Carlo simulations[48].

Conclusion

This article highlighted the importance of orientation of cell and its constituent fibres in functioning of tissue and organ in different ways with specific examples. We have assembled various methods utilizing image processing and engineering techniques to determine these quantities. While this article presented important biological attributes in a simplified manner to be utilized by engineers, we also presented important key aspects of engineering analytical tools and advancements in an explanatory manner to be utilized by non-engineering counterparts.

We have presented that most of the approaches were initially developed for some other engineering use and were later absorbed for analysis in the subject concerned. Though there is a rapid growth of new methods, each method is concerned with an isolated and to the point approach applicable only for a specific needs. These can hardly be interchangeably applied, resulting in a new method better than the previous one but with a limited definite scope. Also, since the process of calculation of orientation itself incorporates different individual tricky problems of acquisition, segmentation and finally

orientation, many researchers have handled critical issues involved at a particular step of the process and have given approaches to resolve them in efficient ways. Therefore, there is a need to integrate all these methods in a more generic solution. We have tried to come up with a comprehensive approach to look at the whole problem in a unified way because there is a need to develop an automated, precise, accurate and robust method that could be exploited and trained for a generic as well as a specific case. Furthermore, this could be extended to develop tools for handy operation by researchers of non-engineering backgrounds.

While we have discussed quantification of actin fibre orientation, how the same method can be applied to determine orientation of ECM collagen fibres, which can be used to quantify the traction on the surface of a biological cell, is one of the future directions of this study.

1. Balaban, N. Q., Schwarz, U. S., Riveline, D., Goichberg, P., Tzur, G., Sabanay, I. and Geiger, B., Force and focal adhesion assembly: a close relationship studied using elastic micropatterned substrates. *Nature Cell Biol.*, 2001, **3**(5), 466–472.
2. Chen, C. S., Mechanotransduction – a field pulling together? *J. Cell Sci.*, 2008, **121**(20), 3285–3292.
3. Engler, A. J., Griffin, M. A., Sen, S., Bönnemann, C. G., Sweeney, H. L. and Discher, D. E., Myotubes differentiate optimally on substrates with tissue-like stiffness pathological implications for soft or stiff microenvironments. *J. Biol.*, 2004, **166**(6), 877–887.
4. Gallant, N. D., Michael, K. E. and García, A. J., Cell adhesion strengthening: contributions of adhesive area, integrin binding, and focal adhesion assembly. *Mol. Biol. Cell*, 2005, **16**(9), 4329–4340.
5. Gillespie, P. G. and Walker, R. G., Molecular basis of mechanosensory transduction. *Nature*, 2001, **413**(6852), 194–202.
6. Polte, T. R., Eichler, G. S., Wang, N. and Ingber, D. E., Extracellular matrix controls myosin light chain phosphorylation and cell contractility through modulation of cell shape and cytoskeletal prestress. *Am. J. Physiol.-Cell Physiol.*, 2004, **286**(3), C518–C528.
7. Schwarz, U. S., Balaban, N. Q., Riveline, D., Bershadsky, A., Geiger, B. and Safran, S. A., Calculation of forces at focal adhesions from elastic substrate data: the effect of localized force and the need for regularization. *Biophys. J.*, 2002, **83**(3), 1380–1394.
8. Wang, H. B., Dembo, M., Hanks, S. K. and Wang, Y. L., Focal adhesion kinase is involved in mechanosensing during fibroblast migration. *Proc. Natl. Acad. Sci.*, 2001, **98**(20), 11295–11300.
9. Banes, A. J., Tsuzaki, M., Yamamoto, J., Brigman, B., Fischer, T., Brown, T. and Miller, L., Mechanoreception at the cellular level: the detection, interpretation, and diversity of responses to mechanical signals. *Biochem. Cell Biol.*, 1995, **73**(7–8), 349–365.
10. Davies, P. F. and Tripathi, S. C., Mechanical stress mechanisms and the cell. An endothelial paradigm. *Circulation Res.*, 1993, **72**(2), 239–245.
11. Hu, Y., Böck, G., Wick, G. and Xu, Q., Activation of PDGF receptor α in vascular smooth muscle cells by mechanical stress. *FASEB J.*, 1998, **12**(12), 1135–1142.
12. Cowan, D. B., Lye, S. J. and Langille, B. L., Regulation of vascular connexin 43 gene expression by mechanical loads. *Circ. Res.*, 1998, **82**(7), 786–793.
13. Xu, F., Beyazoglu, T., Hefner, E., Gurkan, U. A. and Demirci, U., Automated and adaptable quantification of cellular alignment from microscopic images for tissue engineering applications. *Tissue Eng. Part C: Meth.*, 2011, **17**(6), 641–649.
14. Black III, L. D., Meyers, J. D., Weinbaum, J. S., Shvelidze, Y. A. and Tranquillo, R. T., Cell-induced alignment augments twitch force in fibrin gel-based engineered myocardium via gap junction modification. *Tissue Eng. Part A*, 2009, **15**(10), 3099–3108.
15. Bozkurt, A., Deumens, R., Beckmann, C., Damink, L. O., Schügner, F., Heschel, I. and Pallua, N., *In vitro* cell alignment obtained with a Schwann cell enriched microstructured nerve guide with longitudinal guidance channels. *Biomaterials*, 2009, **30**(2), 169–179.
16. Cha, J. M., Park, S. N., Noh, S. H. and Suh, H., Time-dependent modulation of alignment and differentiation of smooth muscle cells seeded on a porous substrate undergoing cyclic mechanical strain. *Artificial Organs*, 2006, **30**(4), 250–258.
17. Geckil, H., Xu, F., Zhang, X., Moon, S. and Demirci, U., Engineering hydrogels as extracellular matrix mimics. *Nanomedicine*, 2010, **5**(3), 469–484.
18. Kapoor, A., Caporali, E. H., Kenis, P. J. and Stewart, M. C., Microtopographically patterned surfaces promote the alignment of tenocytes and extracellular collagen. *Actabiomaterialia*, 2010, **6**(7), 2580–2589.
19. Etemad-Moghadam, B., Guo, S. and Kemphues, K. J., Asymmetrically distributed PAR-3 protein contributes to cell polarity and spindle alignment in early *C. elegans embryos*. *Cell*, 1995, **83**(5), 743–752.
20. Ritchie, A. C., Wijaya, S., Ong, W. F., Zhong, S. P. and Chian, K. S., Dependence of alignment direction on magnitude of strain in esophageal smooth muscle cells. *Biotechnol. Bioeng.*, **102**(6), 1703–1711.
21. Wolinsky, H. and Glagov, S., Structural basis for the static mechanical properties of the aortic media. *Circ. Res.*, 1964, **14**(5), 400–413.
22. Wang, W., Itoh, S., Konno, K., Kikkawa, T., Ichinose, S., Sakai, K. and Watabe, K., Effects of Schwann cell alignment along the oriented electrospun chitosan nanofibres on nerve regeneration. *J. Biomed. Mater. Res. Part A*, 2009, **91**(4), 994–1005.
23. Li, Y., Huang, G., Zhang, X., Wang, L., Du, Y., Lu, T. J. and Xu, F., Engineering cell alignment *in vitro*. *Biotechnol. Adv.*, 2014, **32**(2), 347–365.
24. De, R. and Safran, S. A., Dynamical theory of active cellular response to external stress. *Phys. Rev. E*, 2008, **78**(3), 031923.
25. Nagayama, K., Kimura, Y., Makino, N. and Matsumoto, T., Strain waveform dependence of stress fibre reorientation in cyclically stretched osteoblastic cells: effects of viscoelastic compression of stress fibres. *Am. J. Physiol.-Cell Physiol.*, 2012, **302**(10), C1469–C1478.
26. Helm, P., Beg, M. F., Miller, M. I. and Winslow, R. L., Measuring and mapping cardiac fibre and laminar architecture using diffusion tensor MR imaging. *Ann. NY Acad. Sci.*, 2005, **1047**(1), 296–307.
27. Lehmkuhl, D. and Sperelakis, N., Electronic spread of current in cultured chick heart cells. *J. Cell. Comp. Physiol.*, 1965, **66**(1), 119–133.
28. Yang, Z., Tao, J., Wang, J. M., Tu, C., Xu, M. G., Wang, Y. and Pan, S. R., Shear stress contributes to t-PA mRNA expression in human endothelial progenitor cells and nonthrombogenic potential of small diameter artificial vessels. *Biochem. Biophys. Res. Commun.*, 2006, **342**(2), 577–584.
29. Lee, M. H., Wu, P. H., Staunton, J. R., Ros, R., Longmore, G. D. and Wirtz, D., Mismatch in mechanical and adhesive properties induces pulsating cancer cell migration in epithelial monolayer. *Biophys. J.*, 2012, **102**(12), 2731–2741.
30. Tilghman, R. W., Cowan, C. R., Mih, J. D., Koryakina, Y., Gioeli, D., Slack-Davis, J. K. and Parsons, J. T., Matrix rigidity regulates cancer cell growth and cellular phenotype. *PLoS ONE*, 2010, **5**(9), e12905.

31. Afridi, M. J., Liu, C., Chan, C., Baek, S. and Liu, X., Image segmentation of mesenchymal stem cells in diverse culturing conditions. In *IEEE Winter Conference on Applications of Computer Vision* 2014, pp. 516–523.
32. Huang, L. K. and Wang, M. J. J., Image thresholding by minimizing the measures of fuzziness. *Pattern Recognition*, 1995, **28**(1), 41–51.
33. Li, C. H. and Tam, P. K. S., An iterative algorithm for minimum cross entropy thresholding. *Pattern Recognition Lett.*, 1998, **19**(8), 771–776.
34. Kapur, J. N., Sahoo, P. K. and Wong, A. K., A new method for gray-level picture thresholding using the entropy of the histogram. *Comput. Vision, Graphics, Image Proc.*, 1985, **29**(3), 273–285.
35. Otsu, N., A threshold selection method from gray-level histograms. *Automatica*, 1975, **11**(285–296), 23–27.
36. Shanbhag, A. G., Utilization of information measure as a means of image thresholding. CVGIP: *Graph. Models Image Proc.*, 1994, **56**(5), 414–419.
37. Yen, J. C., Chang, F. J. and Chang, S., A new criterion for automatic multilevel thresholding. *IEEE Trans. Image Proc.*, 1995, **4**(3), 370–378.
38. Ng, C. P., Hinz, B. and Swartz, M. A., Interstitial fluid flow induces myofibroblast differentiation and collagen alignment *in vitro*. *J. Cell Sci.*, 2005, **118**(20), 4731–4739.
39. Lee, A. A., Graham, D. A., Cruz, S. D., Ratcliffe, A. and Karlon, W. J., Fluid shear stress-induced alignment of cultured vascular smooth muscle cells. *J. Biomechan. Eng.*, 2002, **124**(1), 37–43.
40. Meijering, E., Cell segmentation: 50 years down the road (life sciences). *IEEE Sig. Proc. Mag.*, 2012, **29**(5), 140–145.
41. Wu, Q., Merchant, F. and Castleman, K., Microscope Image Processing, Academic Press, 2010, Ch. 8, pp. 113–157.
42. Bengtsson, E., Wahlby, C. and Lindblad, J., Robust cell image segmentation methods. Pattern Recognition and Image Analysis C/C of Raspoznavaniye Obrazov I Analiz Izobrazhenii., 2004, **14**(2), 157–167.
43. Haris, K., Efstratiadis, S. N., Maglaveras, N. and Katsaggelos, A. K., Hybrid image segmentation using watersheds and fast region merging. *IEEE Trans. Image Proc.*, 1998, **7**(12), 1684–1699.
44. Calderero, F. and Marques, F., Region merging techniques using information theory statistical measures. *IEEE Trans. Image Proc.*, 2010, **19**(6), 1567–1586.
45. Lin, Z., Jin, J. and Talbot, H., Unseeded region growing for 3D image segmentation. In *Selected Papers from the Pan-Sydney Workshop on Visualisation*, Australian Computer Society, Inc., Darlinghurst, Australia, 2000, vol. 2, pp. 31–37.
46. Bayan, C., Levitt, J. M., Miller, E., Kaplan, D. and Georgakoudi, I., Fully automated, quantitative, noninvasive assessment of collagen fibre content and organization in thick collagen gels. *J. Appl. Phys.*, 2009, **105**(10), 102042.
47. Dehghan, N., Payvandy, P. and Tavanaie, M. A., Nano fibre images thresholding based on imperial competitive algorithm. *Int. J. Comput. Appl.*, 2014, **99**(6), 37–41.
48. Marquez, J. P., Fourier analysis and automated measurement of cell and fibre angular orientation distributions. *Int. J. Solids Struct.*, 2006, **43**(21), 6413–6423.

Received 9 June 2015; revised accepted 21 July 2016

doi: 10.18520/cs/v111/i12/1936-1945